*J. Fluid Mech.* (1997), *vol.* 336, *pp.* 69–90



# Cessation of screech in underexpanded jets

By GANESH RAMAN

NYMA Inc., Experimental Fluid Dynamics Section, NASA Lewis Research Center Group, Brook Park OH 44142, USA

(Received 11 April 1996 and in revised form 24 October 1996)

In significantly underexpanded jets, screech inherently ceases to exist. This paper studies screech cessation in a supersonic rectangular jet and provides an explanation for its occurrence. Experimental data are presented for fully expanded Mach numbers, $M_j$, ranging from 1.1 to 1.9. Screech becomes unsteady beyond $M_j = 1.65$ and ceases to exist beyond $M_j = 1.75$. The reason for this cessation has remained a mystery, and this paper examines three suspects: (i) the theory of a frequency mismatch between screech tones and the band of the most-amplified jet instability waves, (ii) the notion that Mach disk formation disrupts the shock-cell structure and weakens the screech-producing shocks, and (iii) the idea that acoustic feedback and receptivity diminish at high levels of underexpansion. A thorough interrogation of experimental data shows that (i) is not the main cause of screech cessation here, (ii) plays an insignificant role, and (iii) appears to have been largely responsible for screech cessation. Cessation occurs because feedback to the jet lip is diminished due to excessive expansion of the jet boundary. Further, since the jet lip now reflects and scatters low intensity sound, the end result is poor receptivity at the initial shear layer. This theory is substantiated by the re-activation of screech when the nozzle lip thickness is made larger than the expanded jet boundary. Finally, increasing lip thickness is seen to produce a systematic shift (to higher $M_j$) of the onset of cessation. The results of this study are of direct relevance to the sonic fatigue problem in aircraft structures, because understanding screech helps prevent such damage.

## 1. Introduction

Screech tones are emitted by imperfectly expanded jets under certain conditions. A better understanding of screech is useful for tailoring exhaust nozzle designs to minimize fatigue failure of aircraft components. Pioneering work on screech was done by Powell (1953*a*, *b*), followed by Lassiter & Hubbard (1954), Hammitt (1961), Davies & Oldfield (1962*a*, *b*), and Glass (1968). According to Powell (1953*a*, *b*) the resonant screech loop depends on several factors including the growth of instability waves in the shear layer, their interaction with the shock-cell structures to produce a tone, and the subsequent feedback of the tone to the jet lip. Extensive summaries of screech and other components of jet noise are available in review papers by Fisher & Morfey (1976), Seiner (1984), and Tam (1991, 1995).

Despite several years of progress, our understanding of screech is incomplete, and screech amplitudes cannot be predicted without recourse to empiricism. Screech amplitude is unpredictable because screech depends on a multitude of parameters and is often intermittent and unsteady. Screech unsteadiness (under certain conditions) was reported by Powell (1953*a*, *b*), Lassiter & Hubbard (1954), Davies & Oldfield (1962*a*, *b*), and Harper-Bourne & Fisher (1974). Harper-Bourne & Fisher (1974)

encountered screech unsteadiness when studying broadband shock-associated noise that is inevitably accompanied by screech. The presence of steady screech itself was a problem since screech can suppress broadband shock associated noise (Norum 1984). The problem was further aggravated when screech became unsteady and caused uncertainties in the measurement of broadband shock-associated noise. As a result of this problem Harper-Bourne & Fisher (1974) explored methods for reducing and steadying screech and found that it could be made steady (and dominant) by the addition of a reflector plate upstream of the nozzle exit. A further point made by Harper-Bourne & Fisher (1974) was that when the reflector plate was covered with acoustic foam, the screech amplitude was reduced but remained steady. Additional work on the use of reflectors and lip thickeners to modify screech was done by Poldervaart, Wijnands & Bronkhurst (1973), Norum (1983, 1984) and Ponton & Seiner (1992).

Given this background, focus now turns to the present problem, i.e. the issue of screech cessation in significantly underexpanded jets. As the fully expanded jet Mach number, $M_j$, is increased screech becomes unsteady beyond $M_j = 1.65$ and ceases to exist beyond $M_j = 1.75$. In the present work the phenomenon of 'cessation' is documented and an explanation is provided for its occurrence. The paper examines three probable causes for screech cessation: (i) Tam's theory (Tam, Ahuja & Jones 1994; Tam 1995) that a mismatch between screech frequency and the frequency of the most-amplified instability waves leads to a significant reduction of screech amplitude, (ii) the possibility that the Mach disk disrupts the shock spacings and reduces the strength of shocks that are responsible for screech generation, and (iii) diminished feedback and receptivity.

The present experimental data and linear stability analysis indicate that (i) only played an indirect role in cessation. The Mach disk (ii) did not reduce the shock strengths or alter shock spacings significantly enough for cessation to occur. It was found that excessive expansion of the jet boundary blocked feedback to the jet lip. Further, since the jet lip reflected and scattered low-intensity sound, the end result was poor receptivity at the initial shear layer. Thus, (iii) was the main contributor to cessation. This paper offers a detailed examination and a step-by-step reasoning for the cessation phenomenon. It is believed that the data and findings are of significant scientific value in modelling feedback and receptivity over the entire Mach number range. The final goal would be to stimulate and guide the development of better screech prediction models for designing jet nozzles that minimize the fatigue failure of aircraft components.

## 2. Experimental apparatus and procedure

### 2.1. *Continuous flow supersonic jet facility*

The experiments were carried out at the NASA Lewis Research Center Jet Facility shown in figure 1. The 76 cm diameter plenum tank was continuously supplied with compressed air at pressures up to 875 kPa (125 Psig) at 26.7 °C (80 °F). After passing through a filter that removed dirt and dust, air entered the plenum axially where it was laterally distributed by a perforated plate and a screen. Two circumferential splitter rings that contained acoustic treatment (kevlar) removed upstream valve noise. The flow was further conditioned by two 50-mesh screens before exiting into the room through the rectangular nozzle shown in figure 2(*a*). The rectangular jet nozzle included a circular-to-rectangular transition section, and a converging nozzle contour, all integrated into one piece. The nozzle contour and dimensions are depicted in figure

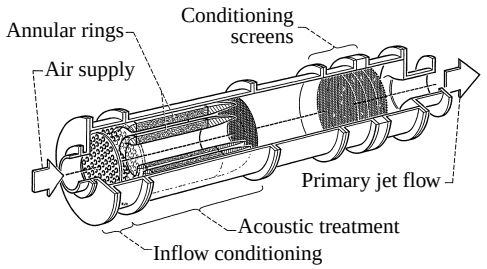


FIGURE 1. Supersonic jet facility.

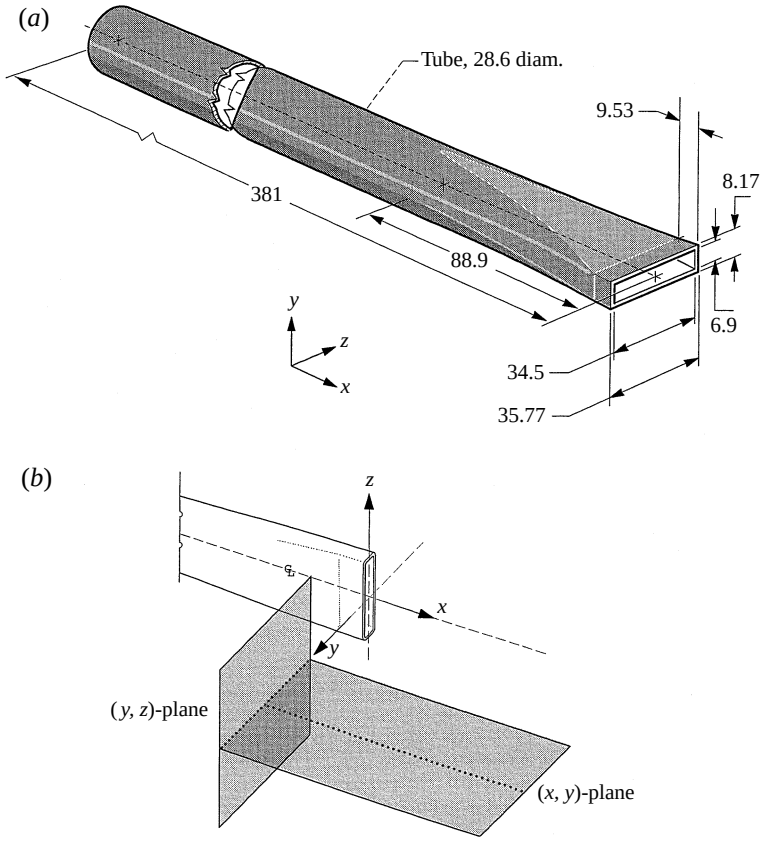


FIGURE 2. Rectangular jet nozzle and measurement planes. (*a*) Nozzle with dimensions in mm. (*b*) Measurement planes for near-field acoustics.

2(*a*). An automatic feedback control system was used to maintain constant air-supply conditions. The control system could restrict pressure variations during each run to within 0.2%. Such precise control was essential for this experiment since the screech tone was extremely sensitive to changes in operating conditions.

The nozzles, the probe traversing mechanism, and other reflective surfaces in the near field were covered with two layers of acoustically absorbent open-cell polyurethane foam (0.635 cm thick uncompressed) to minimize strong reflections from the nozzles and plenum. The material is known to be very effective in absorbing incident sound in the frequency range of 1000–25000 Hz (with several layers, it can also absorb lower frequencies).

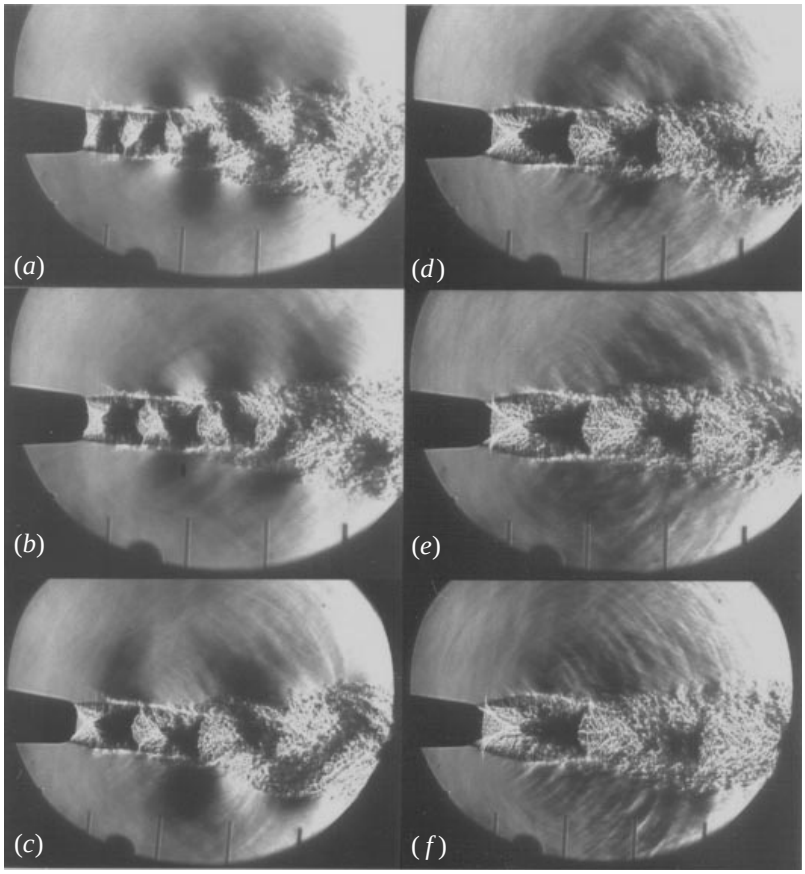


FIGURE 3. Spark schlieren photographs of the narrow dimension of rectangular jets at various levels of underexpansion. (*a*) $M_j = 1.2$, (*b*) 1.3, (*c*) 1.4, (*d*) 1.5, (*e*) 1.6, (*f*) 1.7.

### 2.2. *Measurement techniques*

A spark schlieren system was used for flow visualization. The system included a Palflash light source, a microscope objective, two spherical mirrors (15.24 cm diameter, 91.44 cm focal length), and a vertical knife-edge. The light source consisted of an electric arc in an inert atmosphere of argon gas; it could produce a 1 μs pulse of high intensity light (4 J). Photographs were taken by allowing light from the knife-edge to fall directly on Polaroid film.

The acoustic measurements were made using 0.64 cm ($\frac{1}{4}$ in.) diameter B&K microphones mounted on a three-dimensional traversing mechanism for the near-field noise surveys. The noise measurement planes are shown in figure 2(*b*). The B&K microphones were omnidirectional within $\pm 1$ dB up to 10 kHz and within $\pm 3$ dB up to 20 kHz. The microphones were calibrated using a B&K pistonphone calibrator, with corrections for day-to-day changes in atmospheric pressure. The sound pressure levels reported in this paper are in dB relative to 20 μPa. The acoustic data were recorded using a B&K analyser, and transient events were captured using a Spectral Dynamics instrument.

A short dual-cone static pressure probe designed by Pinckney (1975) at NASA Langley and used previously by Norum & Seiner (1982) was used for the static pressure measurements in the jet. Because the static pressure rises sharply downstream of a

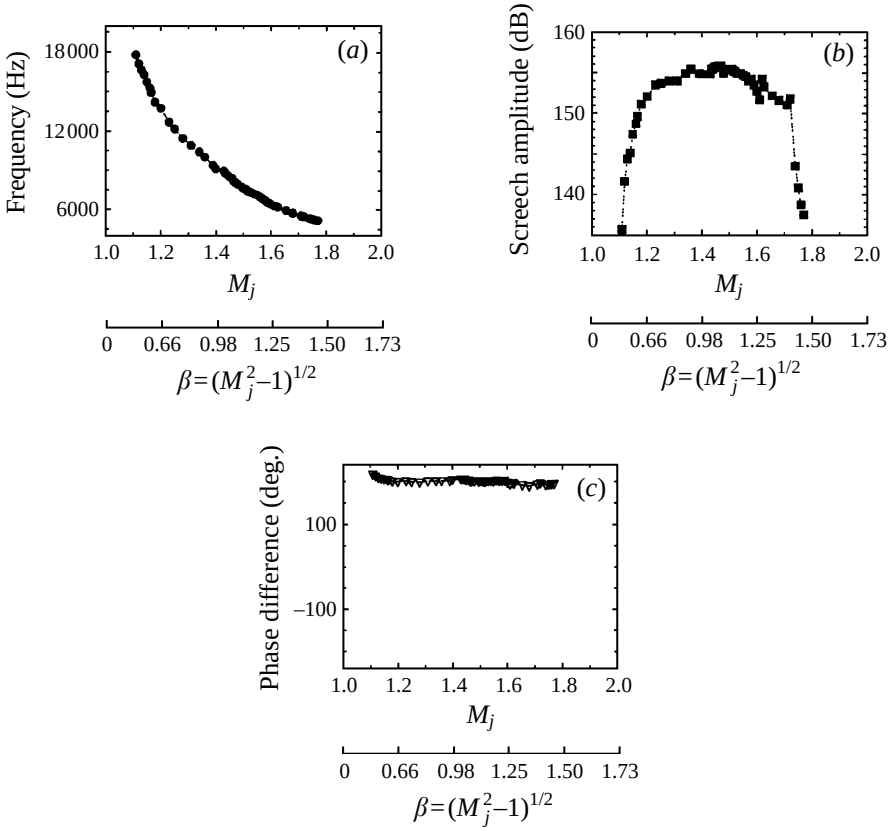


FIGURE 4. Screech tone characteristics at various levels of underexpansion. Microphones were located at $x = 0$, $z = 0$ and were separated by $\Delta y = 2h$. (*a*) Screech frequency versus the fully expanded jet Mach number. (*b*) Screech amplitude versus the fully expanded jet Mach number. (*c*) Phase difference between microphones on either side of the jet's narrow dimension versus the fully expanded jet Mach number.

shock, the static pressure probe could be used to detect Mach disk formation as well as shock spacing and strength. Despite errors caused by the obtrusive probe, shock spacings obtained from the static pressure probes agreed reasonably well with those determined using schlieren. Hence, the shock spacings and strengths obtained using the Pinckney (1975) probe are reasonably accurate for the present purpose.

## 3. The phenomenon of screech cessation

Cessation occurs in significantly underexpanded jets when screech inherently ceases to exist. This study documents this phenomenon in detail before offering reasons for its occurrence. The spark schlieren photographs in figure 3 illustrate the evolution of the jet with an increase in the fully expanded Mach number. The focus for the present discussion is the absence of jet oscillation and the strong near-acoustic field (visible as alternate dark and light regions outside the jet boundary) at high jet Mach numbers. A pair of microphones located at the nozzle lip, on either side of the nozzle's smaller dimension gathered the data presented in figure 4(*a–c*). As the Mach number increased the screech frequency decreased (figure 4*a*) because of the increase in shock cell

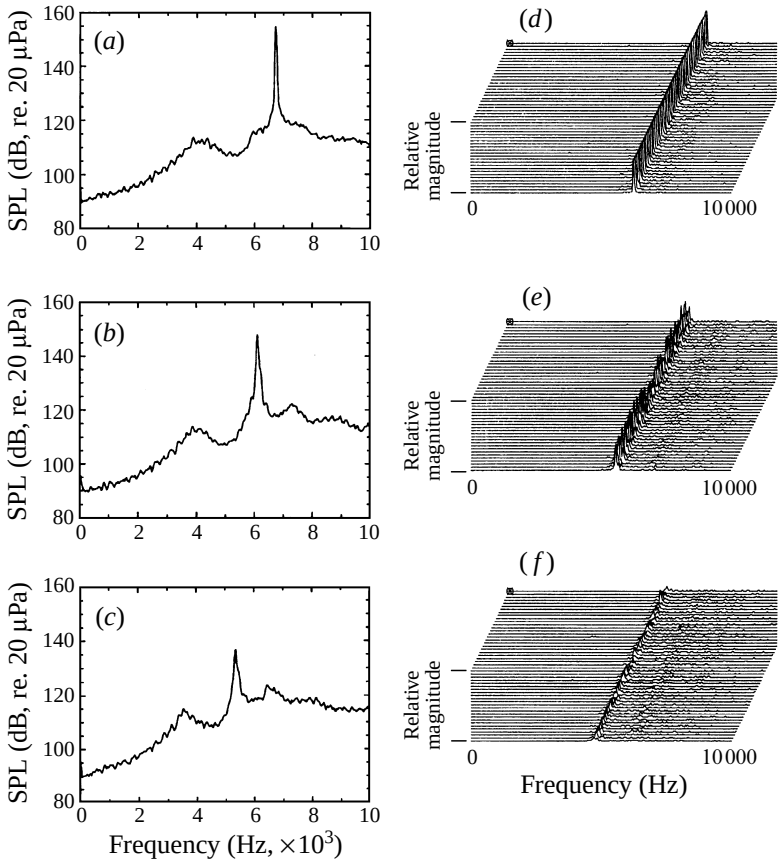


FIGURE 5. Evaluation of screech unsteadiness at high levels of underexpansion by contrasting time-averaged spectra with a waterfall plot of instantaneous spectra. Spectra are from a microphone located at $x = 0$, $y = h$, $z = 0$. ($a$, $d$) $M_j = 1.6$; ($b$, $e$) 1.65; ($c$,$f$) 1.75.

spacing, which caused an increase in the wavelength of screech and consequently a decrease in the screech frequency. Figure 4($b$) shows a plot of the screech tone amplitude measured at the nozzle lip versus the fully expanded jet Mach number. Our focus here will be on the fall-off of the amplitude beyond $M_j = 1.65$, and the reason for its occurrence. The phase difference between the two microphones placed on either side of the jet is shown in figure 4($c$). A constant phase difference of 180° indicates that the sinuous mode is prevalent over the entire Mach number range. Note also that there are no mode switches or auxiliary modes over the entire Mach number range. Such mode switches are present in circular jets (Davies & Oldfield 1962$a$, $b$) and in rectangular convergent-divergent bevelled nozzles (Raman 1997).

To characterize unsteadiness during the fall-off in amplitude, this study compares time-averaged spectra in figure 5($a$–$c$) to 'instantaneous spectra' in figure 5($d$–$f$) for $M_j = 1.6$, 1.65 and 1.75. Walker, Gordeyev & Thomas (1995) used the Wavelet transform to address the intermittency issue that is addressed here using instantaneous spectra. The instantaneous spectra were obtained by performing a fast Fourier transform (FFT) of smaller segments (with a 40% overlap) from a long time sequence (4.816 s). The FFT block size was 1024 and the sampling rate was 25.6 KHz, providing spectral data in the range from 0 to 10 KHz with a frequency bandwidth of 25 Hz. The result is displayed as a waterfall plot of 'instantaneous spectra'. The instantaneous

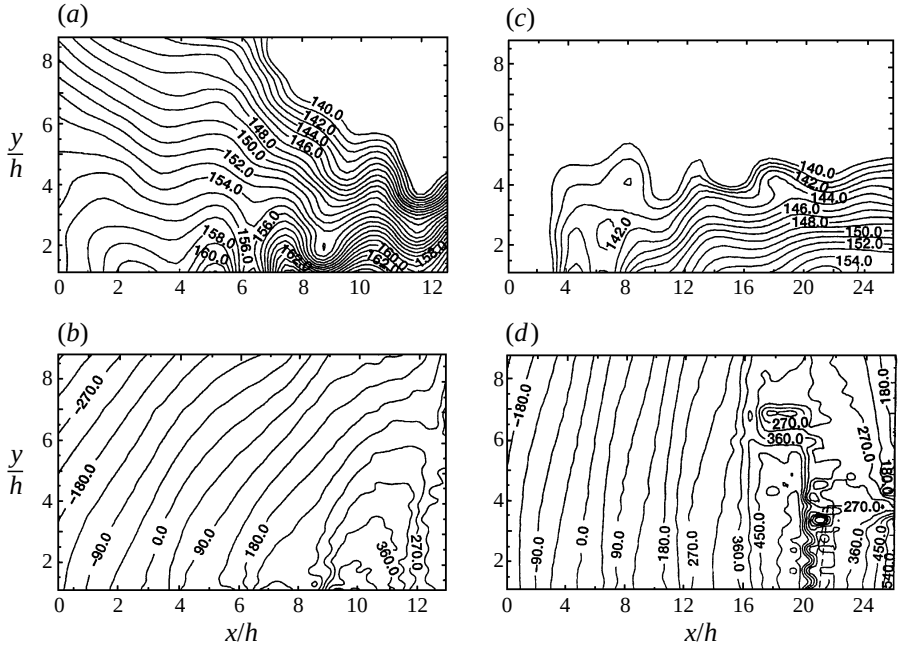


FIGURE 6. Amplitude and phase of the screech tone in the $(x, y)$-plane at $z/h = 0$: $(a, c)$ sound pressure levels (dB); $(b, d)$ isophase contours (degrees). $(a, b)$ $M_j = 1.45$. $(c, d)$ $M_j = 1.75$.

spectra indicate that screech becomes unsteady beyond $M_j = 1.65$ and is barely perceptible at $M_j = 1.75$.

A detailed documentation at two Mach numbers will now be provided: one case in which screech is very strong ($M_j = 1.45$) and the other representing the onset of cessation ($M_j = 1.75$). Screech amplitude and relative phase information on the $(x, y)$-plane are provided for the two cases in figure 6(*a–d*). Low sound pressure level (SPL) contours (below 140 dB) are not shown in the figure. The amplitude information (figure 6*a*, *c*) indicates that the sources were much stronger for the $M_j = 1.45$ case and that high sound pressure levels reached the nozzle lip ($x/h = 0$, where $h$ is the smaller nozzle dimension). In contrast, for the $M_j = 1.75$ case the source strength was weaker and the sound pressure levels dropped considerably before reaching the nozzle lip. At both Mach numbers the amplitude data (figure 6*a*, *c*) show the existence of a standing wave pattern, and this pattern is stronger for the $M_j = 1.45$ case (figure 6*a*). Upstream-propagating acoustic waves and downstream-propagating hydrodynamic waves combine to form the standing wave pattern. Such standing waves in the near field of screeching jets have been observed by several researchers (Davies & Oldfield 1962*a*, *b*; Westley & Wooley 1969, 1975; Chan 1972; and more recently by Rice & Taghavi 1992 and Panda 1996). The following paragraph discusses the use of a wavelength that is derived from the standing wave to normalize the data. The isophase contours (figure 6*b*, *d*) indicate that the directivity of screech is different for the two cases under consideration.

A cut along the centre of figure 6(*a*) is shown for several Mach numbers in figure 7(*a*), and warrants two comments. First, when the data are normalized by the wavelength of the standing wave ($1/\lambda_s = 1/\lambda_a + 1/\lambda_h$, where $\lambda_s$, $\lambda_a$, and $\lambda_h$ are wavelengths of the standing, acoustic, and hydrodynamic waves, respectively – Panda 1996) the maxima and the minima of all curves are aligned. The standing wave

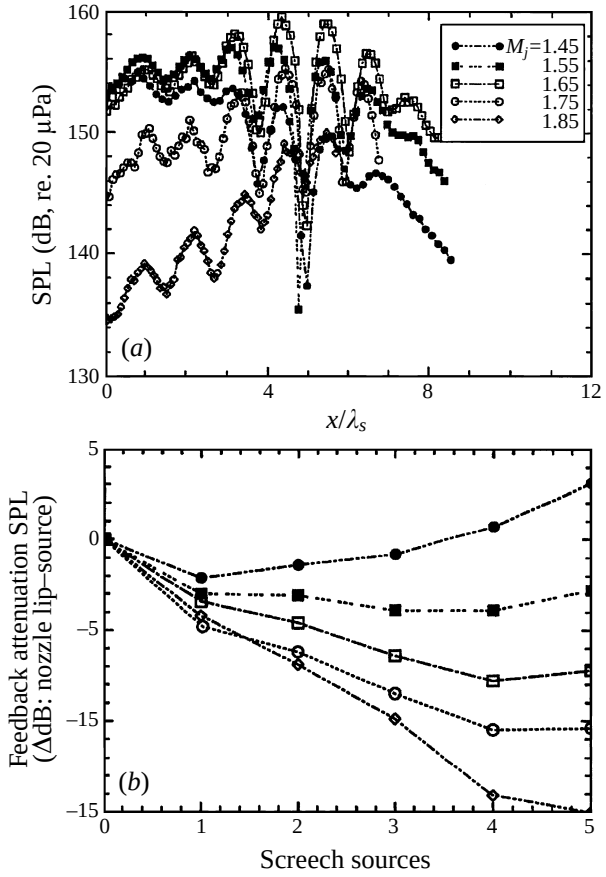


FIGURE 7. Acoustic feedback characteristics for various levels of underexpansion. (*a*) Axial variation in screech sound pressure levels, $y/h = 5$, $z/h = 0$. (*b*) Feedback attenuation.

calculation used the measured frequency and the ambient speed of sound (for $\lambda_a$); a phase velocity ($c/U_j$) of 0.55 was used to calculate $\lambda_h$. Secondly, for the screech cessation cases ($M_j = 1.75$, 1.85), the amplitude of screech drops significantly before reaching the nozzle lip. The latter point (i.e. feedback attenuation) is examined by calculating the difference in sound pressure level between levels measured at the nozzle lip and those measured at the apparent sources. For the first five apparent sources seen as peaks in figure 7(*a*), the feedback attenuation is shown in figure 7(*b*) for various levels of underexpansion. It is clear that feedback methodically attenuates when underexpansion increases, with more efficient feedback occurring at lower jet Mach numbers.

Acoustic amplitude and phase contours for $M_j = 1.45$ and 1.75 on the $(y, z)$-plane are shown in figure 8. The amplitude data show that the peak amplitude occurred at the jet lip for the $M_j = 1.45$ case, whereas it occurred away from the lip for $M_j = 1.75$. The phase data indicate that a null region exists where the phase does not change for both cases. However, the null region is larger for $M_j = 1.75$. The data and analysis given in figure 9 indicate that this null region and phase variation can be easily modelled using a theory that was used earlier to explain the synchronization of multiple supersonic jets (Rice 1995; Raman & Taghavi 1996).

The phase variation model (see figure 9*a*) invokes several assumptions. First, the

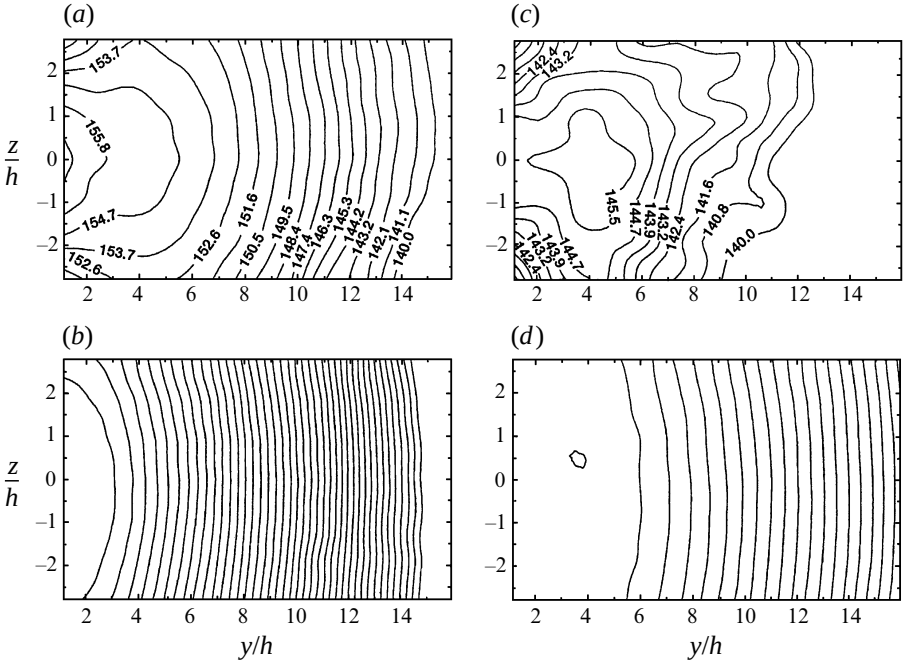


FIGURE 8. Amplitude and phase of the screech tone in the $(y, z)$-plane at $x/h = 0$: $(a, c)$ sound pressure levels (dB), $(b, d)$ isophase contours (contour interval of 12 degrees). $(a, b)$ $M_j = 1.45$, $(c, d)$ $M_j = 1.75$.

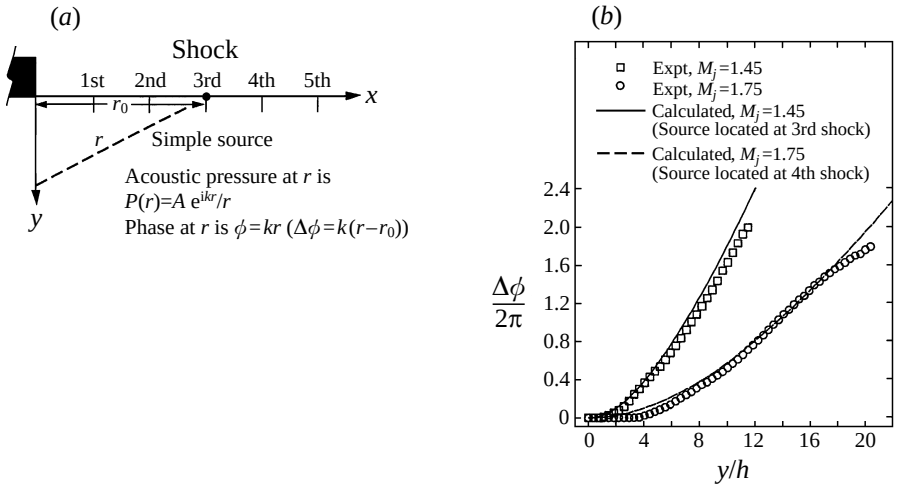


FIGURE 9. Measured and calculated relative phase in the transverse ($y$) direction, $x/h = 0$, $z/h = 0$. ($a$) Schematic describing relative phase calculation. ($b$) Comparison of experimental and theoretical values.

multiple sources of screech are replaced by a single 'equivalent source'. Secondly, the source is located at $y = h/2$, where the tip of the shock interacts with the coherent eddies to produce sound. Finally, as illustrated in figure 9($a$), it is assumed that the source radiates as a simple source, and the acoustic pressure at any point, $r$, is $P(r) = A\,e^{ikr}/r$, where $A$ is the amplitude, $k = 2\pi/\lambda$, $\lambda$ = acoustic (screech) wavelength. The phase in the $y$-direction at the nozzle exit is simply $\phi = kr$, and it follows that $\Delta\phi =$

$k(r-r_0)$. This simple theory is compared with the experiment in figure 9(*b*). The best match is obtained if the source is located at the third shock at $M_j = 1.45$, and at the fourth shock at $M_j = 1.75$. The screech source shift from the third to the fourth shock occurs because, at higher $M_j$, the amplification of instability waves at the screech frequency is lower; however, the wave still grows but peaks further downstream, thus producing the downstream screech source shift.

It is important to note that the equivalent source idea is not in conflict with Powell's (1953*a*, *b*) multiple source representation. Although there are numerous sources, the effective source centre depends on only one or two shock cells depending on the jet Mach number. The dominant acoustic centre being at shock three (Krothapalli *et al.* 1986; Kaji & Nishijima 1996) or four is not difficult to explain because near the jet exit the shock strengths are very high, but the instabilities are still growing there. Far downstream the shock strengths diminish and the jet's coherent stucture is also subject to dissipation. In other words when the multiple source array displays a clear acoustic centre, the phase variation in the *y*-direction at the nozzle exit plane can be modelled assuming that there is a single equivalent source.

## 4. Possible causes of screech cessation

Figure 10 allows us to evaluate the possible causes for screech cessation by reviewing the mechanisms which are operating in a resonant screech loop. First the instability waves grow; then they interact with the shocks to produce sound. This sound propagates upstream and is then reflected and scattered by the lip, producing a broad spectrum of wavelengths that facilitates the coupling (receptivity) of hydrodynamic waves in the shear layer with the external acoustic waves (Morkovin 1969; Rogler & Reshotko 1975). A disruption of any of these processes can precipitate screech cessation. The step-by-step process that follows aims to examine all possible reasons.

### 4.1. *Frequency mismatch theory*

Tam *et al.* (1994) proposed the frequency (wavenumber) mismatch theory to explain the reduced intensity of screech in heated jets. They showed that as the jet's temperature increases, the frequency (band) of the most-amplified instability wave(s) decreases. On the other hand, the screech tone frequencies increased with jet temperature. Based on their stability calculations and experimental data, they concluded that the frequencies of the screech tones and those of the most-amplified instability wave (band) move apart as jet temperature increases. Thus, it is not surprising that the screech tone amplitudes for heated jets are reduced since the screech feedback loops are not driven by the band of the most amplified instability waves. In the remainder of this section this theory will be examined as a possible cause for screech cessation in significantly underexpanded jets.

To examine the 'wavenumber mismatch theory' this study compares linear stability results for the experimental conditions to measured frequencies. The linear stability calculations for cases corresponding to those in the experiments were done in 1996 by A. B. Cain & W. W. Bower at McDonnell Douglas Aerospace (private communication). Only information essential to understand these results will be provided here. For details of the calculation procedure, the reader is referred to Cain *et al.* (1995), and Cain & Bower (1996).

The linear theory deals with small perturbations and linearized equations, so it can only predict the initial growth (locally) of a small perturbation. However, some general insight into the development of large-scale structures in the jet can be obtained by

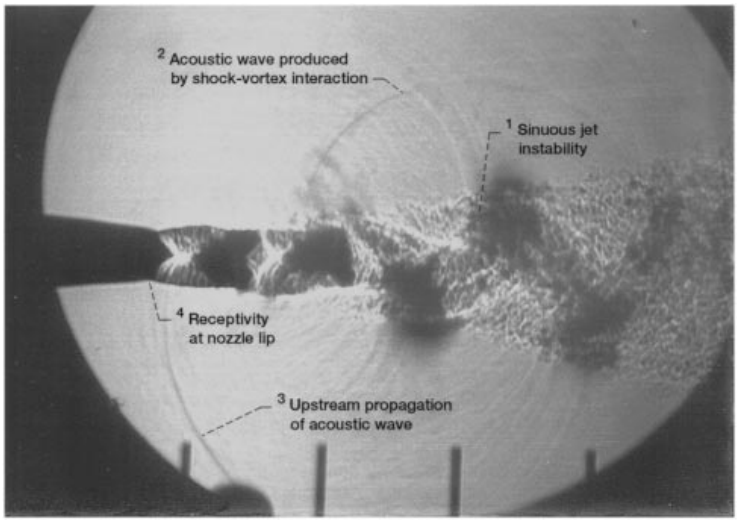


FIGURE 10. Mechanisms operating in a resonant screech loop, $M_j = 1.5$, rod spacing $= 3.5h$.

examining the linear solution. A hyperbolic tangent velocity profile of the following form was used for the calculations:

$$\frac{U}{U_j} = \frac{1}{2}\left[1 - \tanh\left(\frac{y - y_0}{\frac{1}{2}\delta_\omega}\right)\right],$$

where $U$ is the velocity, $U_j$ is the jet exit centreline velocity; $y$ represents the transverse coordinate, $y_0$ the location of the velocity inflection point in the shear layer, and $\delta_\omega$ the vorticity thickness defined as $\delta_\omega = U_{CL}/(\partial U/\partial y)_{max}$, where $U_{CL}$ is the centreline velocity.

The temperature profile used was

$$\frac{T}{T_j} = \frac{T_\infty}{T_j} + \frac{1}{2}\left(1 - \frac{T_\infty}{T_j}\right)\left[1 - \tanh\left(\frac{y - y_0}{\frac{1}{2}\delta_\omega}\right)\right],$$

where $T_j$ is the jet exit centreline temperature, and $T_\infty$ is the free-stream temperature. For the temperature profile, $\delta_\omega$ and $y$ are taken to be the same as those for the velocity profile. Stability calculations at $2y_0/\delta_\omega = 2$ (fully developed region) along with experimentally determined values of a non-dimensional frequency $\omega(\omega = 2\pi f \frac{1}{2}\delta_\omega/U_j$, where $f$ is the frequency in Hz) are shown in figure 11 ($a$, $b$). Figure 11 ($a$) shows the amplification envelope ($\alpha_i \frac{1}{2}\delta_\omega$) versus $\omega$, and figure 11 ($b$) the phase velocity ($C_r$) versus $\omega$, both for the sinuous (antisymmetric) mode in a two-dimensional jet.

Experimental values of $\omega$ were determined using measurements, and operating conditions in the following manner. First, the screech frequency ($f$) was determined using a microphone located at the jet exit (see spectra shown in figure 5 $a$–$c$). Secondly, the nozzle pressure ratio $P_t/P_a$ (where $P_t$ and $P_a$ are the stagnation and ambient pressures, respectively) was used to calculate $M_j$ using $M_j = \sqrt{5[(P_t/P_a)^{(\gamma-1)\gamma} - 1]}$, where $\gamma$ is the ratio of specific heats ($\gamma = 1.4$ for air). Further, $U_j$ was determined using $U_j = M_j \gamma^{1/2} R T_j$, and $T_j$ was calculated using $T_\infty/T_j = 1 + \frac{1}{2}(\gamma - 1) M_j^2$. Note that $T_\infty$ and $T_j$ represent the total (ambient) and static temperatures respectively, and $R$ is the universal gas constant. Finally, for a hyperbolic tangent profile, the vorticity thickness, $\delta_\omega$, can be approximated as $\frac{1}{2}\delta_\omega = (y_{0.5} - y_{0.12})$ where the subscripts refer to fractions of the jet centreline velocity. The values of $\frac{1}{2}\delta_\omega$ at an axial location midway between the

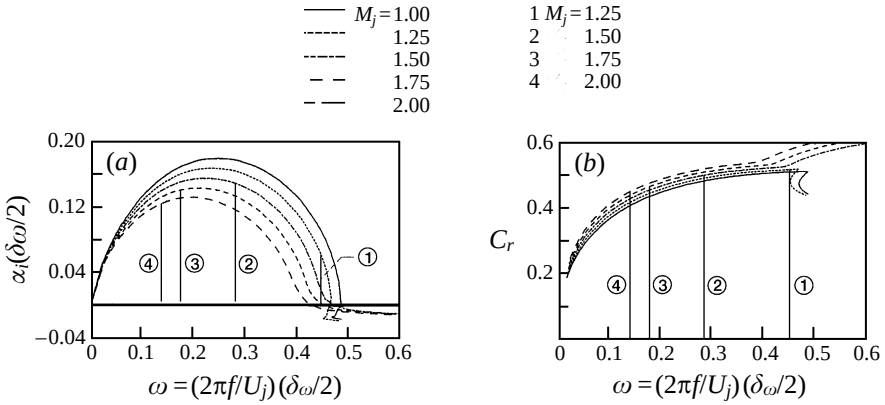


FIGURE 11. Linear stability calculations and comparison with experiment. (*a*) Band of most-amplified instability waves. (*b*) Phase velocity. The curves are results of linear stability analysis (Cain & Bower 1996; Cain *et al.* 1995). The lines 1–4 are experimental data from the present work.

third and fourth shocks were used. Thus, both the stability results and experimental values were scaled consistently to create a meaningful comparison.

Comparison between theory and experiment indicates that although the peak amplification as predicted by the linear theory does diminish with an increase in $M_j$, the decrease is not nearly sufficient to precipitate cessation. The experimentally determined values of $\omega$ decrease in an orderly manner as $M_j$ is increased; a trend also visible in the theory as a shift in the centre of the amplification envelope. Even at $M_j = 2$ (beyond screech cessation), the $\alpha_i(\frac{1}{2}\delta_\omega)$ value in figure 11(*a*) is still quite large, and does not offer adequate cause for screech cessation.

In contrast to the observations reported by Tam *et al.* (1994) for hot jets, in the present case of an unheated rectangular jet, the frequencies of the screech tone and that of the band of most amplified instabilities move in the same direction. When the screech tone weakens, its frequency is well within the amplified instability band. In addition, the amplification rates are of the same order as that for strong screech. Thus, the decrease in peak amplification at higher Mach numbers does not appear to be significant enough to cause cessation. Thus, although the location of the screech frequency within the instability amplification band does play a role, it is not likely to cause screech cessation. Further notes on the disappearance of screech in hot jets appear in Massey *et al.* (1994), Ahuja *et al.* (1994), and Krothapalli & Strykowski (1996).

Some comments on the phase velocity are in order before closing this subsection. The calculated phase velocities for a two-dimensional jet shown in figure 11(*b*) are seen to increase with an increase in $M_j$; a trend also observed in the circular jet experiments of Morrison & McLaughlin (1980). In an ideally expanded circular jet, McLaughlin, Morrison & Troutt (1975) and Morrison & McLaughlin (1980) measured an average phase velocity ($c/U_j$) of 0.65. In contrast, in a shock-containing circular jet, Hu & McLaughlin (1990) measured a $c/U_j$ value of 0.55 that compares well with the value of 0.54 measured by Raman & Rice (1994) in a rectangular jet. A further validation of this number was provided when Tam & Reddy (1993) calculated the broadband shock-associated noise from a rectangular jet by assuming $c/U_j = 0.55$ over the entire $M_j$ range, and obtained favourable agreement with experiment. Finally, the phase velocity can change abruptly when a mode switch occurs in circular jets. However, such a mode switch is absent in the present case of a choked rectangular jet.

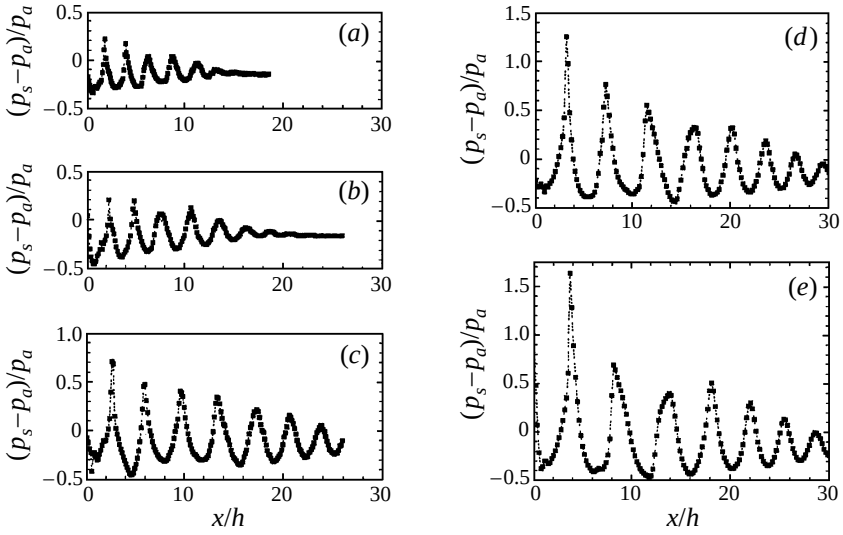


FIGURE 12. Static pressure measured on the jet's centreline for various levels of underexpansion. (*a*) $M_j = 1.45$, (*b*) 1.55, (*c*) 1.65, (*d*) 1.75, (*e*) 1.85.

### 4.2. *Mach disk*

The second theory to be examined here is the possibility that screech cessation at very high Mach numbers is caused by Mach disk formation. The Mach disk theory will first be described briefly followed by a thorough examination in the context of screech cessation. The Mach disk is said to have formed when the end of the first shock cell turns into a normal shock. When the Mach disk forms, the flow downstream of the first shock has mixed subsonic and supersonic regions. Screech cessation could occur if the Mach disk destabilizies the shock-cell structure of the jet or weakens the screech-producing shocks (three and four). Such a destabilization did occur in jets with spanwise oblique shock-cell structures (Raman 1997).

The Mach disk can be detected by taking advantage of the fact that (i) the static pressure rises immediately downstream of a shock, and (ii) this rise will be steeper when the first shock turns into a normal shock. The static pressure measurements on the jet's centreline are shown in figure 12. The initial focus is on the first shock (first pressure rise). The value of the pressure immediately downstream of the first shock increases gradually from $M_j = 1.45$ to 1.65 as the strength of the first shock increases. The static pressure then shoots up between $M_j = 1.65$ and 1.75 (perhaps because the oblique shocks begin to transition into a normal shock), and continues to increase steeply up to $M_j = 1.85$. The shock-cell spacings and strengths of the first four shocks that are derived from the data of figure 12 are shown in figure 13(*a*, *b*). The shock spacings (figure 13*a*) do not exhibit any abnormal trends over the entire Mach number range. The average (of four) shock spacing agrees with the predictions of Morris, Bhat & Chen (1989) and with Tam's (1988) formula based on the Prandtl–Pack (Pack 1950) theory. An explicit comparison is not provided since the objective here is not to check shock spacing theories but to show that the Mach disk formation does not appear to have altered shock spacing trends significantly enough for screech cessation to occur. More importantly, it is seen from figure 13(*b*) that the strengths of shocks three and four are not adversely affected by the formation of the Mach disk. Therefore, there is no logical reason to connect Mach disk formation to screech cessation.

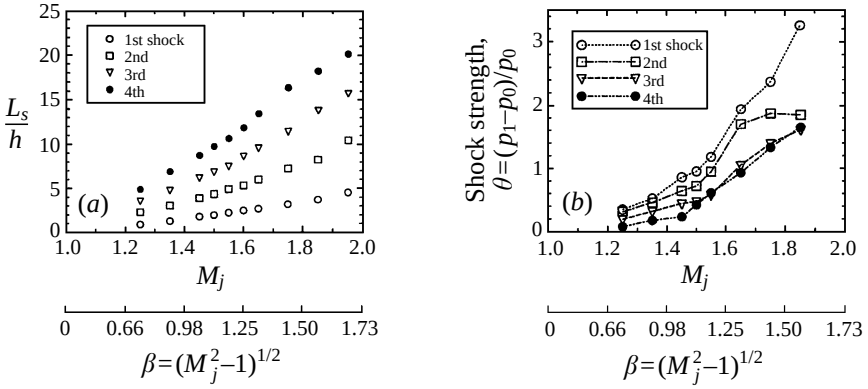


FIGURE 13. (*a*) Shock spacing and (*b*) strength versus the fully expanded Mach number.

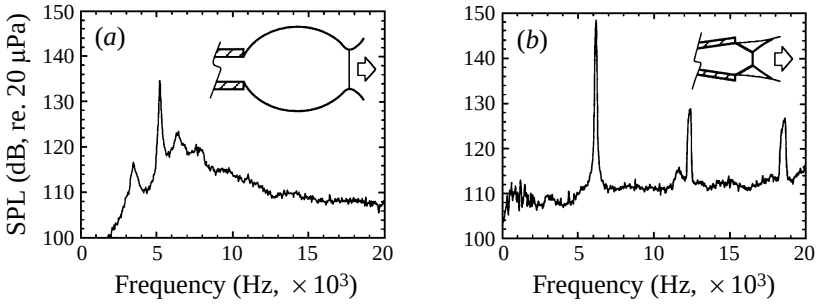


FIGURE 14. Screech under conditions of significant under- and over-expansion. (*a*) Convergent rectangular nozzle used in the present work at $M_j = 1.80$. SPLs measured at $x = 0$, $y = h$, $z = 0$. (*b*) Circular convergent–divergent nozzle ($M_d = 1.8$) operated at $M_j = 1.2$. SPLs measured at $x = 0$, $y = D$.

Another piece of evidence arises if we consider the Mach disks formed for underexpanded and overexpanded conditions. Screech data were taken for the two cases sketched in figure 14(*a*, *b*), both with the same nozzle exit lip thickness ($t/h = 0.69$). Figure 14(*a*, *b*) also shows microphone spectra for the two cases under consideration. As described in § 3, the $M_j = 1.8$ underexpanded jet from a convergent rectangular nozzle exhibits screech cessation (figure 14*a*, screech amplitude = 134 dB). The overexpanded Mach disk case was obtained by operating a circular nozzle with a design Mach number, $M_d = 1.8$, at $M_j = 1.2$. The spectrum in figure 14(*b*) indicates that the jet with an overexpanded Mach disk did produce intense screech (screech amplitude of 148 dB). This section closes with the note that screech cessation occurred in a jet with an underexpanded Mach disk, whereas a jet with an overexpanded Mach disk sustained screech; therefore, it appears that the Mach disk itself is not the cause for screech cessation.

### 4.3. *Diminished feedback and receptivity*

The last idea concerns diminished feedback and receptivity. This paper proposes that the excessive expansion of the jet boundary at higher Mach numbers causes an aerodynamic blockage of feedback at the nozzle lip. Since the sound now impinges on the nozzle lip at a much lower amplitude, the reflection and scattering of sound of a reduced intensity at the lip results in a reduced receptivity in the initial shear layer. Substantiation for this argument follows.

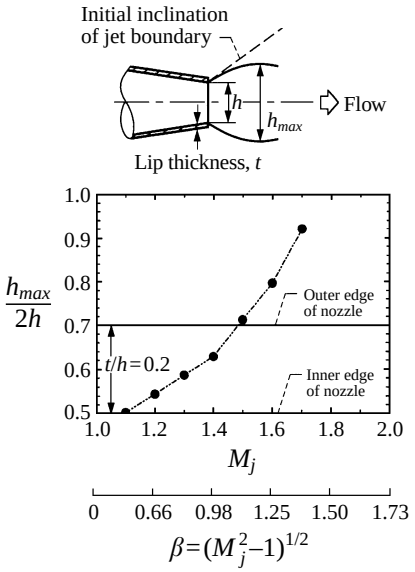


FIGURE 15. Maximum dimension of the jet boundary relative to the nozzle lip thickness.

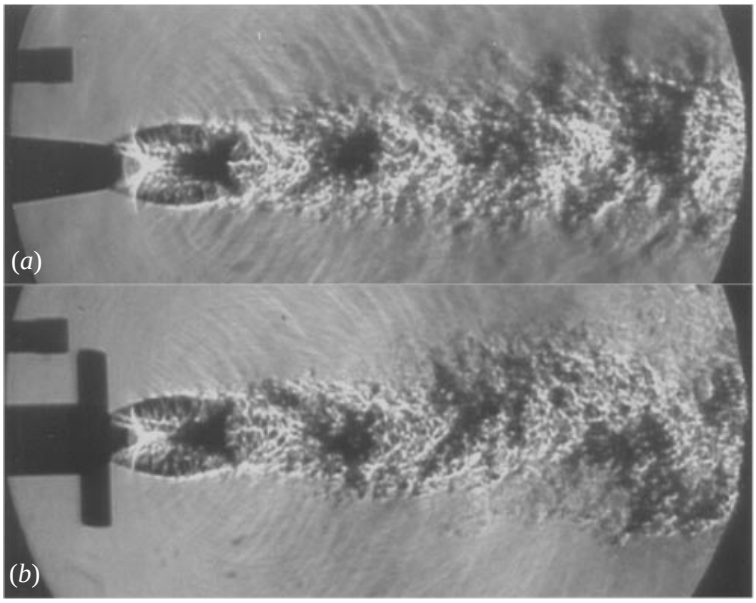


FIGURE 16. Spark schlieren photographs of screech reactivated by thickening the nozzle lip. $M_j = 1.75$; (*a*) $t/h = 0.2$, (*b*) 2.0.

The growth of $h_{max}$ (the fully expanded jet dimension) near the jet exit is shown in figure 15. The $h_{max}$ values shown in figure 15(*b*) were measured from schlieren photographs. The central idea here is that the increase in initial inclination of the 'barrel' shock (referred to as the 'bottle' shock by Crist, Sherman & Glass (1966)) and the growth in $h_{max}$ beyond the nozzle lip, block feedback to the jet lip. The blockage explains the low screech sound pressure levels at the jet exit (figure 8*c*). The above processes first reduce screech and ultimately stop it. Note that the explanation provided here also provides experimental proof for the weakest-link theory of Tam, Seiner & Yu

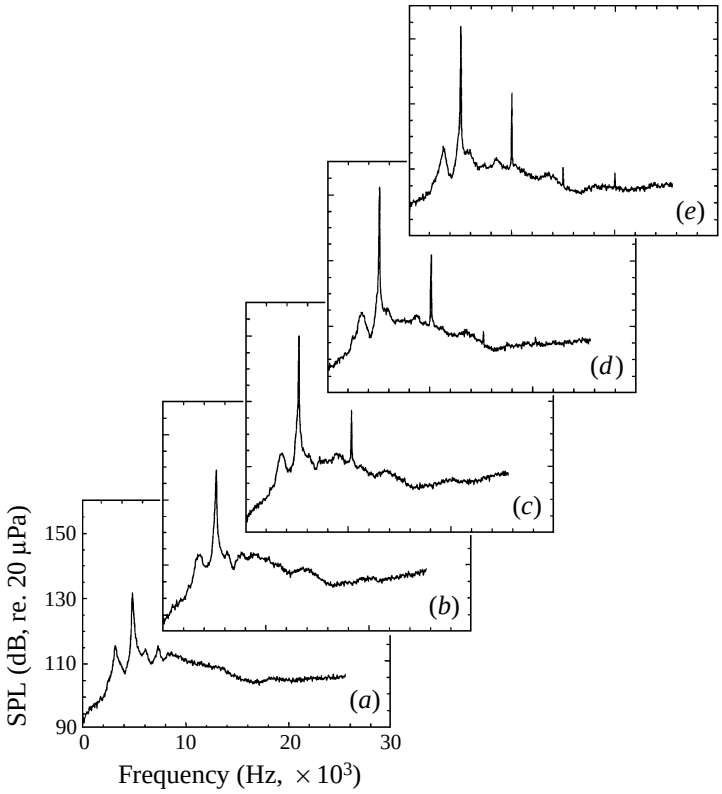


FIGURE 17. Reactivation of screech using nozzle lip thickeners. Microphone at $x = 0$, $y = 3.7h$, $z = 0$; $M_j = 1.75$; (*a*) $t/h = 0.2$, (*b*) 0.5, (*c*) 1.0, (*d*) 1.5, (*e*) 2.0.

(1986). The physical blockage of feedback using acoustic barriers placed at certain locations downstream of the nozzle exit is known to eliminate screech (Poldervaart *et al*. 1973; Ahuja 1984, 1985; Rice & Raman 1993). The difference here is that the barrier is aerodynamic ('barrel' shock), and is located between the nozzle exit and the end of the first shock cell.

If the proposed explanation is correct, then in a case where cessation has occurred we should be able to rekindle screech by thickening the nozzle lip. This is indeed the case, as shown by the spark schlieren photographs in figure 16. The lip thickener with $t/h = 2.0$ is seen to produce a large sinuous oscillation of the jet that is characteristic of strongly screeching jets. The systematic reactivation of screech with increasing lip thickness is evident from the spectra of figure 17. The $t/h = 2.0$ case displays a strong screech tone at a level that is 20 dB higher than the thin-lip ($t/h = 0.2$) case. As regards screech steadiness, the lip thickener made low-amplitude intermittent screech intense and steady. Recall the instantaneous spectra in figure 5(*d–f*): without the lip thickener, the instantaneous spectra resembled that in figure 5(*f*) and with the lip thickener, that in figure 5(*d*). However, in the interest of conciseness the additional instantaneous spectra are not shown here. Several additional points are noted from figure 17. First, the resurrection of screech suppressed broadband shock-associated noise in the frequency range 6000–8000 Hz. This observation is in agreement with that of Norum (1984). Secondly, the weak screech tone at $t/h$ values of 0.2 and 0.5 does not produce a harmonic. This is not surprising since the harmonic is generated by nonlinearities associated with a high-amplitude screech tone. When the lip thickness is increased

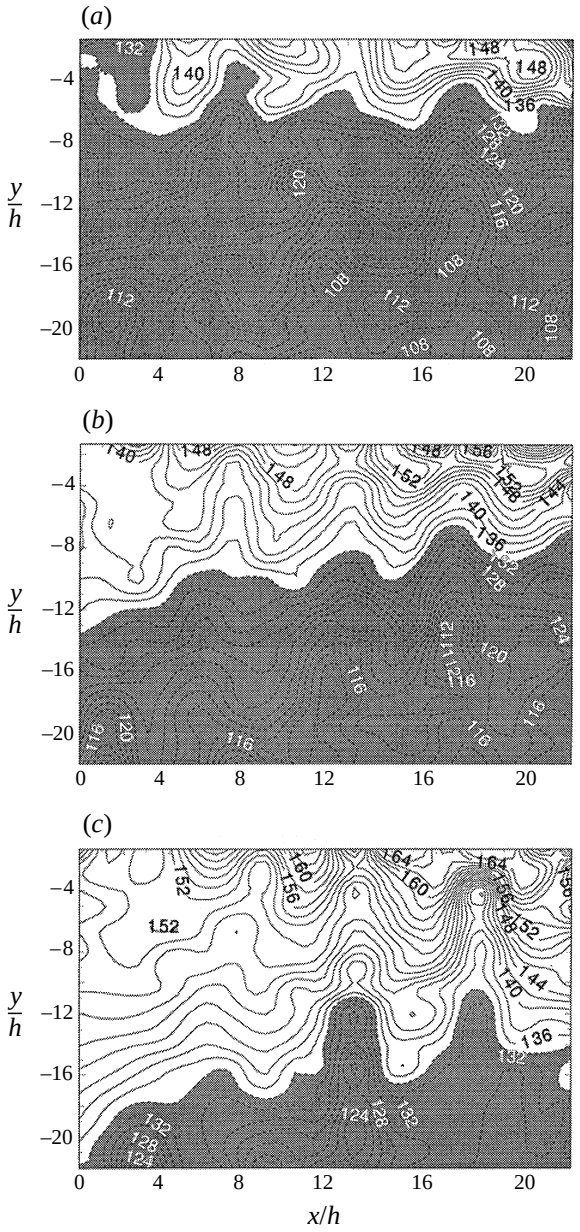


FIGURE 18. Near-field map of screech sound pressure levels for various lip thickeners: $(x, y)$-plane at $z/h = 0$; $M_j = 1.75$; (*a*) $t/h = 0.2$, (*b*) 1.0, (*c*) 2.0. Contour spacing 2 dB, grey area represents levels below 134 dB.

further ($t/h = 1$, 1.5, 2.0) the amplitude of the fundamental screech tone increases and a harmonic emerges. Finally, the lip thickener reactivated screech at the same frequency at which cessation occurred. If wavenumber mismatch had been the reason for screech cessation, reactivation at the same frequency would not have been possible. Thus, the lip thickener effect independently refutes the wavenumber mismatch theory.

Figure 18 shows changes in the entire near field as the nozzle lip is thickened. For the screech cessation case (figure 18*a*) it is seen that high sound pressure levels do not

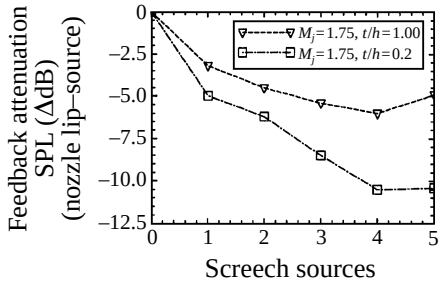


FIGURE 19. Effect of nozzle exit lip thickness on feedback attenuation.

reach the nozzle lip. The lip thickener is seen to reactivate screech and modify the entire near field. The role of the lip thickener in reactivation of screech can be explained as follows. First, the larger nozzle lip now intercepts acoustic waves travelling upstream that would have otherwise been blocked by the excessive expansion of the jet boundary. Secondly, when an acoustic wave is reflected by the thicker nozzle lip, a condition that must be satisfied at the lip surface is that the displacement amplitude should be zero and the pressure amplitude a maximum, which leads to higher sound pressure levels at the nozzle lip. Finally, a thicker nozzle lip scatters and reflects sound. The scattering effect is known (Morkovin 1969; Rogler & Reshotko 1975) to produce a broad spectrum of wavelengths that allows for the coupling of the acoustic and instability waves. In addition, reflection sets up a strong axial standing wave pattern. Tam (1986) showed that a strong axial variation in amplitude can also produce a broad spectrum of wavelengths. Thus, all of the above factors enhance the receptivity of the initial shear layer which leads to the reactivation of screech.

Ponton & Seiner (1992) studied the effect of lip thickness for a choked circular jet from a convergent nozzle. Their data showed that screech which ceased to exist at $M_j = 1.6$ when the lip thickness was $t/D = 0.2$ persisted up to $M_j = 1.9$ when $t/D$ was increased to 0.625. However, the lip thickness effect remained a mystery, and is also complicated by a mode switch from a $C$ mode to a $D$ mode (both helical modes) in their experiments. The present results support the findings of Ponton & Seiner (1992), but they are for rectangular jets where there is only one screech mode (antisymmetric), and there is no mode switch during screech cessation or its revival by lip thickeners; thus the effect of lip thickness is clear.

A comment is in order on changes in feedback due to the lip thickener. Refer back to figure 7(*b*) for a description of feedback attenuation with an increase in the fully expanded jet Mach number. The lip thickening is also seen to decrease feedback attenuation (figure 19) to levels reminiscent of moderately underexpanded jets. A systematic study was also conducted over a range of $M_j$ on the effect of increasing lip thickness on screech cessation (figure 20) after the recognition that lip thickness affects feedback and receptivity. Increase in lip thickness from $t/h = 0.2$ to 2 produces a systematic shift in the onset of cessation to higher $M_j$. For example, screech cessation that occurred beyond $M_j = 1.75$ for a thin-lipped ($t/h = 0.2$) nozzle now occurred only beyond $M_j = 1.9$ for a thick-lipped ($t/h = 2$) nozzle.

In cases where screech cessation had occurred, screech could also be reactivated using an upstream reflector. The upstream axial position had to be re-adjusted (tuned) for strong screech to appear at all values of $M_j$. Although the fact that an upstream reflector can enhance or suppress screech had been known earlier (Harper-Bourne & Fisher 1974; Nagel, Denham & Papathanasiou 1983; Norum 1984), it is interesting to

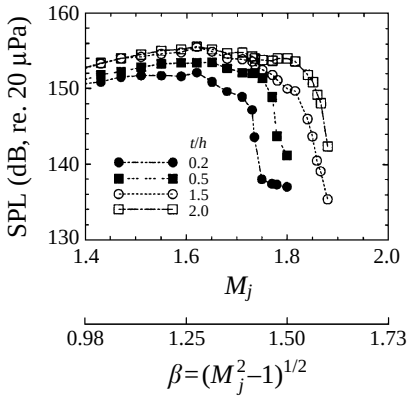


FIGURE 20. Shifting the onset of screech cessation to higher Mach numbers using nozzle lip thickeners. SPLs measured from microphone located at $x = 0$, $y = 3.7h$, $z = 0$.

note here that a non-screeching (shock-containing) jet can be made to screech again using this technique. A detailed description of the mechanism by which a reflector functions is given in Raman, Panda & Zaman (1997).

## 5. Concluding remarks

The phenomenon of natural cessation of screech in highly underexpanded jet flows was examined. Results illuminate the relative importance of various processes that occur in the resonant screech loop. These processes include: growth of instability waves in the shear layer, shock–vortex interactions that produce sound, acoustic feedback to the jet lip, and the receptivity of the initial shear layer to acoustic disturbances. Three probable causes for cessation were examined: (i) the theory of a frequency mismatch between screech tones and the band of the most amplified instabilities, (ii) the notion that Mach disk formation weakens shocks (three and four) that are responsible for producing screech, and (iii) the idea that acoustic feedback and receptivity diminish at significant levels of underexpansion.

It was found that although frequency (wavenumber) mismatch did contribute to cessation, diminished feedback and poor receptivity were largely responsible for cessation, also substantiating the weakest-link theory of Tam *et al.* (1986). The indirect contribution of the wavenumber mismatch arises because at higher Mach numbers the amplification of instability waves at the screech frequency is lower; however, the wave still grows but peaks further downstream, thus producing a downstream shift in the screech source location.

The Mach disk formation plays no significant role in screech cessation; substantiation was provided by the absence of abnormalities in shock spacing or shock strength that could destabilize screech. In addition the Mach disk from an overexpanded jet that begins with a compression at the jet exit sustained screech. The key, however, is the excessive expansion of the jet boundary (barrel shock) that blocks feedback to the jet lip. Since the lip is unable to scatter and reflect sound, poor receptivity results. If the nozzle exit lip is made thicker than the jet boundary, then screech returns. The reactivation of screech occurs because (*a*) the larger nozzle lip now intercepts sound that would have otherwise been blocked, (*b*) the sound pressure is a maximum at the lip surface, and (*c*) scattering by the lip produces a broad spectrum of wavelengths that allows for the coupling of acoustic and instability waves. Thus, all

of the above factors enhance the receptivity of the initial shear layer which leads to the reactivation of screech. Increasing the lip thickness also resulted in a systematic shift of the onset of cessation to higher Mach numbers.

The aerodynamic blocking of feedback by the jet boundary causing cessation and the effect of lip thickness in resurrecting screech point to the criticality of feedback and receptivity in sustaining screech. In the past both feedback and receptivity have been given insufficient emphasis in the study of screech by focusing only on instability wave growth and shock structure, a trend that needs to change. It is believed that the results presented here are useful in stimulating work aimed at producing better models of feedback and receptivity over the entire Mach number range. It is hoped that these models would improve the capability of a screech prediction program that could be used to design nozzles that minimize fatigue failure of aircraft components.

I am deeply grateful to Dr A. B. Cain and Dr W. W. Bower, of McDonnell Douglas Aerospace, for performing the stability calculation described in figure 11. Professor C. K. W. Tam of Florida State University and Dr S. H. Walker of the United States Air Force (Wright laboratory) provided insightful comments. Finally, I thank Dr K. B. M. Q. Zaman, Dr J. Panda, Dr E. Envia, and Dr J. Bridges, at the NASA Lewis Research Center, for stimulating discussions on jet screech.

## REFERENCES

Ahuja, K. K. 1984 Basic experimental study of the coupling between flow instabilities and incident sound. *NASA CR* 3789.

Ahuja, K. K. 1985 Some unique experiments on receptivity. *AIAA Paper* 85-0533.

Ahuja, K. K., Massey, K. C., Tam, C. K. W. & Jones, R. R. 1994 Temperature effects on acoustic interactions between altitude test facilities and jet engine plumes. *AEDC TR*-94-10.

Cain, A. B. & Bower, W. W. 1996 Modeling supersonic jet screech: differential entrainment and amplitude effects. *AIAA Paper* 96-0916.

Cain, A. B., Bower, W. W., Walker, S. H. & Lockwood, M. K. 1995 Modeling supersonic jet screech Part 1: vortical instability wave modeling. *AIAA Paper* 95-0506.

Chan, Y. Y. 1972 A simple model of shock cell noise generation and its reduction. *NRC/NAE* (*Canada*) *Aero. Report LR* 564.

Crist, S., Sherman, P. M. & Glass, D. R. 1966 Study of highly underexpanded sonic jet. *AIAA J.* **4**, 68–71.

Davies, M. G. & Oldfield, D. E. S. 1962*a* Tones from a choked axisymmetric jet. I. Cell structure, eddy velocity and source locations. *Acustica* **12**, 257–266.

Davies, M. G. & Oldfield, D. E. S. 1962*b* Tones from a choked axisymmetric jet. II. The self excited loop and mode of oscillation. *Acustica* **12**, 267–277.

Fisher, M. J. & Morfey, C. L. 1976 Jet noise. *AGARD* Lecture series No. 80, Rhode St. Genése, Belgium.

Glass, D. R. 1968 Effects of acoustic feedback on the spread and decay of supersonic jets. *AIAA J.* **6**, 1890–1897.

Hammitt, A. G. 1961 The oscillation and noise of an overpressure sonic jet. *J. Aero Sci.* **28**, 673–680.

Harper-Bourne, M. & Fisher, M. J. 1974 The noise from shock waves in supersonic jets. Noise mechanisms. *AGARD CP* 131, pp. 11-1 to 11-13.

Hu, T. F. & McLaughlin, D. K. 1990 Flow and acoustic properties of low Reynolds number underexpanded supersonic jets. *J. Sound Vib.* **141**, 485–505.

Kaji, S. & Nishijima, N. 1996 Pressure field around a rectangular supersonic jet in screech. *AIAA J.* **334**, 1990–1996.

Krothapalli, A., Hsia, Y., Baganoff, D. & Karamcheti, K. 1986 The role of screech tones in the mixing of an underexpanded rectangular jet. *J. Sound Vib.* **106**, 119–143.

KROTHAPALLI, A. & STRYKOWSKI, P. J. 1996 Revisiting screech tones: effect of temperature. *AIAA Paper* 96-0644.

LASSITER, L. W. & HUBBARD, H. H. 1954 The near noise field of static jets and some model studies of devices for noise reduction. *NACA TN* 3187.

MASSEY, K. C., AHUJA, K. K., JONES, R. R. & TAM, C. K. W. 1994 Screech tones of supersonic heated free jets. *AIAA Paper* 94-0141.

MCLAUGHLIN, D. K., MORRISON, G. L. & TROUTT, T. R. 1975 Experiments on the instability waves in a supersonic jet and their acoustic radiation. *J. Fluid Mech.* **69**, 73–95.

MORRIS, P. J., BHAT, T. R. S. & CHEN, G. 1989 A linear shock-cell model for jets of arbitrary exit geometry. *J. Sound Vib.* **132**, 199–211.

MORKOVIN, M. V. 1969 Critical evaluation of transition from laminar to turbulent shear layers with emphasis on hypersonically travelling bodies. *AFFDL-TR*-68-149.

MORRISON, G. L. & MCLAUGHLIN, D. K. 1980 Instability process in low Reynolds number supersonic jets. *AIAA J.* **18**, 793–800.

NAGEL, R. T., DENHAM, J. W. & PAPATHANASIOU, A. G. 1983 Supersonic jet screech tone cancellation. *AIAA J.* **21**, 1541–1545.

NORUM, T. D. 1983 Screech suppression in supersonic jets. *AIAA J.* **21**, 235–240.

NORUM, T. D. 1984 Control of jet shock associated noise by a reflector. *AIAA Paper* 84-2279.

NORUM, T. D. & SEINER, J. M. 1982 Measurements of mean static pressure and far-field acoustics of shock containing supersonic jets. *NASA TM* 84521.

PACK, D. C. 1950 A note on Prandtl's formula for the wavelength of a supersonic gas jet. *Q. J. Mech. Appl. Maths* **3**, 173–181.

PANDA, J. 1996 An experimental investigation of screech noise generation. *AIAA Paper* 96-1718.

PINCKNEY, S. Z. 1975 A short static-pressure probe design for supersonic flow. *NASA TN-D* 7978.

POLDERVAART, L. J., WIJNANDS, A. P. J. & BRONKHURST, L. 1973 Aerosonic games with the aid of control elements and externally generated pulses. *AGARD CP*-131, (20) pp. 1–4.

PONTON, M. K. & SEINER, J. M. 1992 The effects of nozzle exit lip thickness on plume resonance. *J. Sound Vib.* **154**, 531–549.

POWELL, A. 1953*a* On the noise emanating from a two-dimensional jet above the critical pressure. *Aeronaut. Q.* **4**, 103–122.

POWELL, A. 1953*b* On the mechanism of choked jet noise. *Proc. Phys. Soc. Lond.* **66**, 1039–1056.

RAMAN, G. 1997 Screech tones from rectangular jets with spanwise oblique shock-cell structures. *J. Fluid Mech.* **330**, 141–168.

RAMAN, G., PANDA, J. & ZAMAN, K. B. M. Q. 1997 Feedback and receptivity during jet screech: influence of an upstream reflector. *AIAA Paper* 97-0144.

RAMAN, G. & RICE, E. J. 1994 Instability modes excited by natural screech tones in a supersonic rectangular jet. *Phys. Fluids* **6**, 3999–4008.

RAMAN, G. & TAGHAVI, R. 1996 Resonant interaction of a linear array of supersonic rectangular jets: an experimental study. *J. Fluid Mech.* **309**, 93–111 (and Corrigendum **326**, 1996, 437).

RICE, E. J. 1995 Jet mixer noise suppressor using acoustic feedback. US Patents 5,325,661 and 5,392,597.

RICE, E. J. & RAMAN, G. 1993 Enhanced mixing of a rectangular supersonic jet by natural and induced screech. *AIAA Paper* 93-3263.

RICE, E. J. & TAGHAVI, R. 1992 Screech noise source structure of a supersonic rectangular jet. *AIAA Paper* 92-0503.

ROGLER, H. L. & RESHOTKO, E. 1975 Disturbances in a boundary layer introduced by low intensity array of vortices. *SIAM J. Appl. Maths* **28**, 431–462.

SEINER, J. M. 1984 Advances in high speed jet aeroacoustics. *AIAA Paper* 84-2275.

TAM, C. K. W. 1986 Excitation of instability waves by sound – a physical interpretation. *J. Sound Vib.* **105**, 169–172.

TAM, C. K. W. 1988 The shock-cell structures and screech tone frequencies of rectangular and non-axisymmetric supersonic jets. *J. Sound Vib.* **121**, 135–147.

TAM, C. K. W. 1995 Supersonic jet noise. *Ann. Rev. Fluid Mech.* **27**, 17–43.

TAM, C. K. W. 1991 Jet noise generated by large-scale coherent motion. In *Aeroacoustics of Flight*

*Vehicles: Theory and Practice*, Vol. 1: *Noise Sources* (ed. H. H. Hubbard). NASA RP 1258, WRDC TR 90-3052, pp. 311–390.

TAM, C. K. W., AHUJA, K. K. & JONES III, R. R. 1994 Screech tones from free and ducted supersonic jets. *AIAA J.* **32**, 917–922.

TAM, C. K. W. & REDDY, N. N. 1993 A prediction method for broadband shock associated noise from supersonic rectangular jets. *AIAA Paper* 93-4387.

TAM, C. K. W., SEINER, J. M. & YU, J. C. 1986 Proposed relationship between broadband shock associated noise and screech tones. *J. Sound Vib.* **110**, 309–321.

WALKER, S. H., GORDEYEV, S. V. & THOMAS, F. O. 1995 A wavelet transform analysis applied to unsteady jet screech resonance. In *High Speed Jet Flows* (ed. G. Raman, S. Kaji & C. Freitas). ASME FED, Vol. 214, pp. 103–108.

WESTLEY, R. & WOOLLEY, J. H. 1969 The near field sound pressures of a choked jet during a screech cycle. Aircraft engine noise and sonic boom. *AGARD CP* 42, pp. 23-1 to 23-13.

WESTLEY, R. & WOOLLEY, J. H. 1975 The near field sound pressures of a choked jet when oscillating in the spinning mode. *AIAA Paper* 75-479.